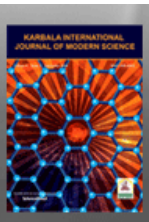

Karbala International Journal of Modern Science

Volume 7 | Issue 3 Article 6

Adaptive reconstruction of the heterogeneous scan line ETM+ correction technique

Heba Kh. Abbas
Department of Physics, College of Science for Women, University of Baghdad, Baghdad, Iraq,
Hebaka_phys@csw.uobaghdad.edu.iq

Salema S. Salman
Department of Clinical Laboratory Science, College of Pharmacy, University of Baghdad, Iraq,
salma3_sultan@copharm.uobaghdad.edu.iq

Rash Awad Abtan
Department of Computer, College of Basic Education, University of Al-Mustansiriyah, Rash_Awad@gmail.com

Anwar H. Al-Saleh
Department of Computer Science, College of Science, University of Mustansiriyah, Baghdad, Iraq,
Anwar.h.m@uomustansiriyah.edu.iq

Ali A. Al-Zuky
Department of Physics, College of Science, University of Mustansiriyah, Baghdad, Iraq,
Prof.alialzuky@uomustansiriyah.edu.iq

Recommended Citation

Abbas, Heba Kh.; Salman, Salema S.; Awad Abtan, Rash; Al-Saleh, Anwar H.; and Al-Zuky, Ali A. (2021) "Adaptive reconstruction of the heterogeneous scan line ETM+ correction technique," *Karbala International Journal of Modern Science*: Vol. 7 : Iss. 3 , Article 6.
Available at: https://doi.org/10.33640/2405-609X.3121

Adaptive reconstruction of the heterogeneous scan line ETM+ correction technique

Abstract

ETM+ is a land-imaging sensor with great and wide use in many fields, however, after May 2003, because of a technical defect in the sensor´s system scan line corrector SLC, it started giving images of earth containing black gap lines at a 22% rate. These gaps made the process of analyzing and extracting accurate information from these images difficult and complicated. Therefore, scientists have developed many techniques to remove the gap lines from all ETM+ band-images and complete the missing data. In this study, three different ETM+ time images with a 16-day interval between them were used to fill gap lines, complementing the images, and minimize the effect of the gaps. However, the adopted temporal filtration method was not able to completely remove the gaps. An added algorithm is used, which is based on using one of three filters (mean, median, and max.) to work on a vertical linear window whose center is on the points of the gap lines in the images. The quality of the resulting images was evaluated using the Jaccard metric standard to find the degree of similarity between the original images and the images that resulted from the implementation of the algorithm, the results showed good quality images, and the gaps were completely removed from the resulting images. A higher degree of similarity was obtained from implementing the (mean and median), ranging between 0.6568 and 0.9007, compared with the (max), where the similarity ranged between 0.6246 and 0.8820. This study aims to fill the images gaps using the temporal filtering technique.

Keywords

Landsat ETM+, Gap filling, Heterogeneous

1. Introduction

Landsat program can be defined as a worldwide land-imaging mission managed via cooperation endeavors between the United States geological surveys (USGS) & the National aeronautic & space administrations (NASA), aiming to provide continuous, worldwide, high resolutions and multispectral information for educational & scientific purposes. Landsat data were utilized in a wide range of earth science activities such as hydrological works as part of a continuous 4 decades-long satellite launching mission [1,2], vegetation dynamics [1,3], land-cover assessments [1], and climate change impacts [1,4]. The satellites have been effective in deriving records of long-term land surface changes, variable and feature description, along with their radiometric and high geometric accuracy. Large parts of the Earth surface displayed on web mapping services like Google Maps, MSN Maps, or Yahoo! Maps are based on Landsat 7 imagery. The scan line corrector (SLC) on Landsat 7's enhanced thematic mapper plus (ETM+) sensor, its purpose is to compensate for the forward motion (along-track) of the spacecraft so that the resulting scans are aligned parallel to each other. Without SLC, the images of the Earth are taken in a "zig-zag" fashion, resulting in some areas being imaged twice and others not imaged at all. unfortunately, SLC failed on 31/05/2003, influencing the fidelity and continuity of the records of internationally important high resolutions satellite (USGS, 2003). Several methods were developed to fill the data gaps. These methods are generally grouped into two categories: geostatistical and deterministic interpolations. The deterministic interpolation methods differ from geostatistical methods by using un-scanned pixel prediction depending on some empirically specified mathematical equations, whereas the geostatistical interpolation procedures incorporate some randomness to make predictions depending upon the image's statistical properties. Below is a list of the methods developed to fill the data gaps:

- USGS (2004) [5] proposed a method called the Local Linear Histogram Matching. This procedure needs input scenes to include snow−cover, minimal clouds, lower temporal variability, and minimal date separation, such a method is not practical in some cloudy areas.
- Maxwell et al. (2007) [6] Introduced a model to fill the gaps based on a multiscale segment. The model is most suitable for homogenous areas, as it cannot depict the properties of a more heterogeneous landscape.
- Pringle et al. (2009) [7] suggested the geostatistical interpolation for the purpose of filling gaps, recommending a co-kriging algorithm for predicting missing values. There must be 2 input images temporally close to the target image, this approach's usability is reduced when the availability of temporally close gap-free imagery is limited. Additionally, the implementation of the geostatistical methods is generally based upon the stationary spatial process assumption, which is not plausible in places where the land cover is expected to dynamically change in time as well as space.
- Chen et al. (2011) [8] have developed the neighborhood similar pixel interpolator (NSPI). This method took both temporal and spatial changes in its consideration instead of considering spatial correlations alone, and NSPI showed more accuracy in recovering missing pixels, particularly for heterogeneous regions. The deterministic NSPI linear interpolators are unable to provide statistical uncertainty to every prediction, which effectively influence its application's robustness.
- Zeng et al. (2013) [9] suggested integrated recovery methods that combine the multi-temporal approaches and non-reference methods for filling the Landsat 7 gaps. In this method, the weighted linear regression (WLR) algorithm was first applied to fill the unscanned pixels, then by the application of the non-reference Laplacian prior regularization method (LPRM), used for filling gap pixels which cannot be predicted by WLR. The integrated method showed an accurate prediction of the missing pixels, particularly in the sharp edges, which assist in retaining the shapes of ground objects. However, it can fail when there are gaps that are too large.
- Mareithoz & Renard, (2010) [10] introduced the direct sampling (DS) method, which is a multiple-point geostatistical topic. The concept of direct sampling is simple as it tries to find a pattern similar to the target patterns, the searching process is directed by Covariate information. It was

https://doi.org/10.33640/2405-609X.3121

formerly used to fill the gaps in a satellite-based Earth observation [11].

- Malambo and Heatwole (2016) [12] presented the profile based interpolators (PBI), which is a k-nearest-neighbor method, as a new method to fill nonstationary data gaps, which was shown to forecast abrupt changes in good accuracy. Additionally, it needs no cloud-free scene, and it can predict the missing value of any date at any position when there are available long sufficient sequential images. However, this method recreates some unwanted data like the image's cloud shadows.
- Scaramuzza et al. (2018) [13] introduced in their study, the local linear histogram-matching, which uses corrective biases and gains depending on the local non-missing pixel.
- Salema et al. (2020) [14] used a correlation coefficient between Landsat ETM+ images before and after scan line corrector failure to fill the gap.

In this study, three different ETM+ temporal images of Baghdad city with a 16-day interval between them were used, where the temporal image averaged method was used to reduce gap lines. Usually, this technique does not completely remove the image gap lines. The main idea of this work is the complete removal of the gap lines from the images that were previously filtered using the temporal method, by adopting spatial filters that are applied locally only to the locations of the remaining gap lines to complete the entire gap removal process. The spatial filtering will be performed on a vertical linear window centered on the points of the gap lines in the image. Finally, the quality of the resulting image correction process will be studied using Jaccard similarity criteria that measure the similarity between the two original (three **temporal images)** and results in an image from algorithms spatial filtering.

2. Landsat SLC- images

The gaps in SLC-off images can be reconstructed by applying both easy linear/nonlinear filters and using spatial interpolation strategies on the malfunctioning ETM+7 image itself. Interpolations may be the strategies of choice when filling data gaps in ETM+ imagery. There are several interpolation techniques like the inverse distance-weighted procedures, splines, and triangulation methods. The USGS EROS Data Center nowadays makes use of these [15,16] techniques in cases where the interpolation is utilized in SLC-off imagery. Limitations of this approach are that greater order derivatives are now not continuous across the facets of the triangles and that if the property adjustments significantly dominate over a quick distance, there will be some oscillations to shut the vertices [17]. Most significantly, this approach does not take full advantage of the spatial facts in the image. On the other hand, spatial independence does not often occur in photography scenes and there is spatial dependence of variability in images, reflected in the digital variety variability (digital number DN) values [17]. The adjacent pixels tend to be auto-correlated spatially and two adjoining pixels will usually be predicted to be of greater similarity in their DN values than would 2 pixels separated by larger distances [17]. Since spatial structures take place in remotely sensed images and DN does not act uniformly across landscapes, appreciation of the magnitude and pattern in spatial variability is essential for the precise interpolation of the missing pixels in the ETM+ imagery. The geostatistical methods established & developed by Georges Matheron in France in the 1960s are designed for spatial statistics and take full benefit of spatial correlation information. Those methods may be applied for discovering and describing spatial patterns and differences in remotely sensed information.

2.1. Image filters

Filters are often used to smooth the images, remove noise, or removing linear or limited point defects, and among the most important known traditional filters are the median filter, the maximum value filter, mode filter, and mean filter. These filters are as follows:

2.2. Mean filter

In the current method, the corrupted image average value in the formerly determined region is calculated using this filter, and then the average value replaces the intensity of the center pixel. The method is repeated to all pixels in degraded images. There is a similarity between this algorithm and the low-pass filter algorithms. The restored image pixel values at each point (x, y) simply represent the arithmetic "mean" estimated by applying pixels in the area defined by S. It is utilized [18] as follows:

$$\widehat{f}(x,y)=\frac{1}{m\times n}\sum_{(s,l)\in S_{xy}} g(s,l) \tag{1}$$

2.3. Median filter

The median filter method is moving the pixel via the image pixels, while every value is replaced by the median value of the neighboring pixels. The pattern of neighboring pixels & their dimensions is known as the window, which moves pixel to pixel through entire images. The median filter is the best well-known order-statistics filter that function's to replace the pixel's values via the median grey-level value in the neighborhood of those pixels [18,19]:

$$\widehat{f}(x,y) = \underset{(s,l)\in S_{xy}}{median}\{g(s,l)\} \quad (2)$$

2.4. Maximum filter

In this filter, the maximum value of the surrounding corrupted pixels is calculated in an image, this value then replaces corrupted pixel intensity. This method is repeated to all pixels in degraded images [18,19].

$$\widehat{f}(x,y) = \max_{(s,l)\in S_{xy}} \{g(s,l)\} \quad (3)$$

2.5. Jaccard image quality metric

There are many quality standards for testing the efficiency and quality of digital images, and the standards differ according to the various uses and applications of the images, and the most important known criterion is the MSE (Mean Square Error), PSNR (Peak Signal to Noise Ratio), In this paper, the mean pairwise Jaccard coefficient, J (f, g) is adopted as the performance metric. The J (f, g) is measuring the similarity and diversity between pairs of objects, and is formulated [20] as follows:

$$J(f,g) = \frac{|f \cap g|}{|f \cup g|} = \frac{|f \cap g|}{|f| + |g| - |f \cap g|} \quad (4)$$

where f & g are the original and processing images respectively. The J (f, g) is defined as the value between 0 & 1, where (0) represents no overlapping, and (1) represents perfect matching.

2.6. Metric similarity

Jaccard similarity measures the similarity between two images the original (three **temporal images)** and the resulting image from the first processing IEi (reduction gap) and between the original (three **temporal images)** and the resulting image from the second processing INi (removed gap) using (mean, median and max) filters by taking the intersection of both and dividing it by their union. The similarity value is then calculated from:

$$Similarity\ value = Jaccard\ index \times 100\% \quad (5)$$

3. Methodology and algorithms

Several methods for overcoming the 2003 failure of the Landsat 7 enhanced thematic mapper plus (ETM+) scan line corrector (SLC) have been introduced. In this study, satellite images ETM+ from 2004 were adopted, where the line width of the gap from up to down is heterogeneous, therefore, the process is adopted to fill gaps using linear and non-linear filters.

3.1. Software and tools

The location of the study area is in the middle part of Iraq, at Landsat world reference system (WRS-84) path 169, row 037, three True-color bands (5, 4, and 3) with 7671 × 7811 image pixels, as shown in Fig. (1). A Landsat 7 ETM+ SLC-off image, acquired on June 12, 2004, was chosen to apply the algorithm. Images of Landsat ecosystem disturbance adaptive processing system (LEDAPS) were taken from the USGS website (http://glovis.usgs.gov). The intruded algorithms of this study were achieved using the algorithms of MatLab software - 2018.

3.2. Study area with image satellite

To observe the effect on varying influences of Landsat cover heterogeneity when performing the gap-filling procedure, a sub-image was once extracted from ETM+7 data (1263 × 1639) pixel. The investigations

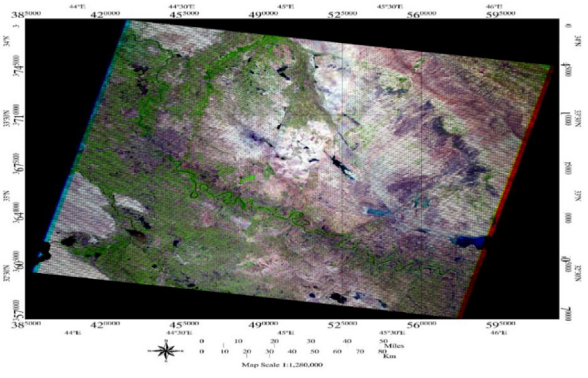

Fig. 1. True color (Near-infrared, red and green) band composites of Landsat ETM+.a- SLC − off image acquired in (June- 2004).

were performed in Baghdad province in the middle part of Iraq at 33.312805 latitudes and 44.361488 longitudes as shown in Fig. (2). It represents a fertile mudslides land area, about 445 km north of Basra, 350 km southeast of Mosul, 320 km southeast of Erbil. The study area is surrounded by palm groves and orchards below the bushes, which are full of fruit-bearing trees such as citrus, as seen in the considerable harvested land.

3.3. The introduced methods for Landsat gap filling

The gap lines of Landsat 7 SLC- off are not uniform in width from left to right, they are wider on the left side and gradually taper towards the right side as shown in Fig. (3a) i.e. ($w_1 > w_3$). To reduce the gap line error, three temporal images are used over a 32-day period, where the used mask filter can reduce the width of gap lines to less than (w_2), so it can enhance all regions of gap width (w) to less than (w_2), while in the left side of the image the gap width ($w > w_2$) does not completely reduce the gap line which is partially enhanced. Fig. (3) shows the results of the proposed technology for 2004 (see Fig. 4).

It is observed from the figure that the algorithm fails to fill all the gap lines, therefore, a new technique has been proposed in this study to completely remove the gap lines.

The introduced algorithm to reduce the gaps:

- Input 3 temporal images IE_i (T_{1i}, T_{2i}, and T_{3i}) for ($i = 1 \rightarrow 7$), where i represents band index.
- Output 3 temporal image without gap line (enhanced) [IN_{1imean}, $IN_{2i\ median}$., and $IN_{3i\ max}$]

1. Calculate the maximum image intensity from the three-input temporal bands.
2. $IE_i = \max(T_{1i}, T_{2i}, T_{3i})$. Where i = 1, 7.
3. Convert IE_6 to binary by using the formula:

$$IE_{B6} = \begin{bmatrix} 1 & if\ IE_6 \geq th \\ 0 & if\ IE_6 < th \end{bmatrix}$$

4. To include all points below and above the gap lines, apply the immediate command for IE_{B6}
5. Calculate a new image IN_i using:

$$IN_i = IE_{B6} \times IE_i \qquad where\ i = 1,2,3,4,5,7,$$

6. For each pixel in IN_i equal to zero ($P_0 = 0$), take five pixels above and below $P_0 = 0$
7. Apply adaptive (median, mean, max) vector filters [VP (11×1)].
8. Replace the value of $P_0 = 0$ with the value of the adaptive (median, mean, max) filter.

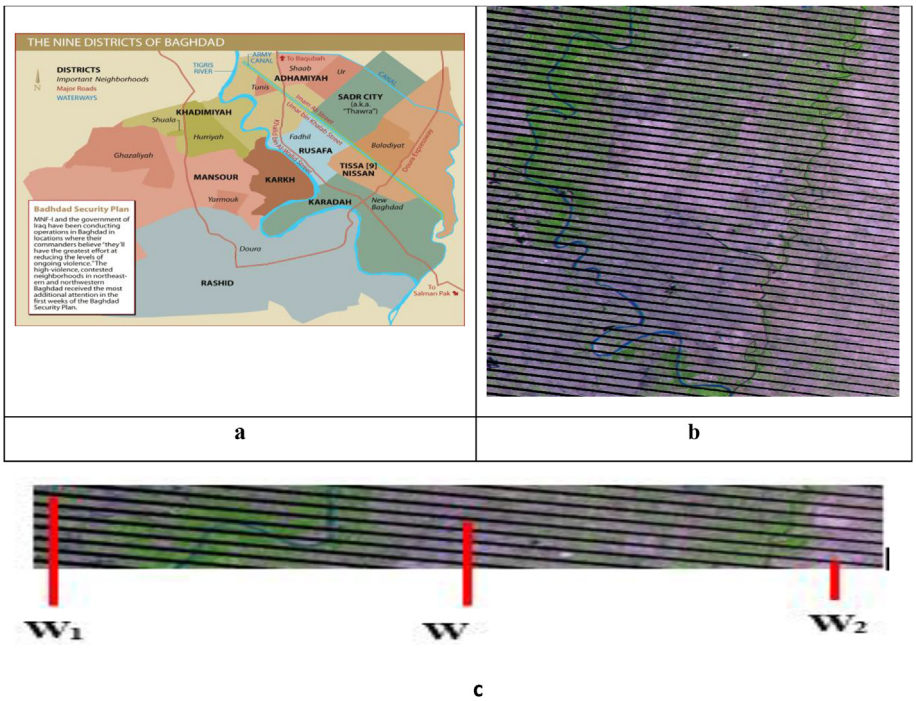

Fig. 2. a-Administrative map of Baghdad city districts and b-Photomap Landsat ETM_+ of the study area c- Photo of SLC – off are not of equal width.

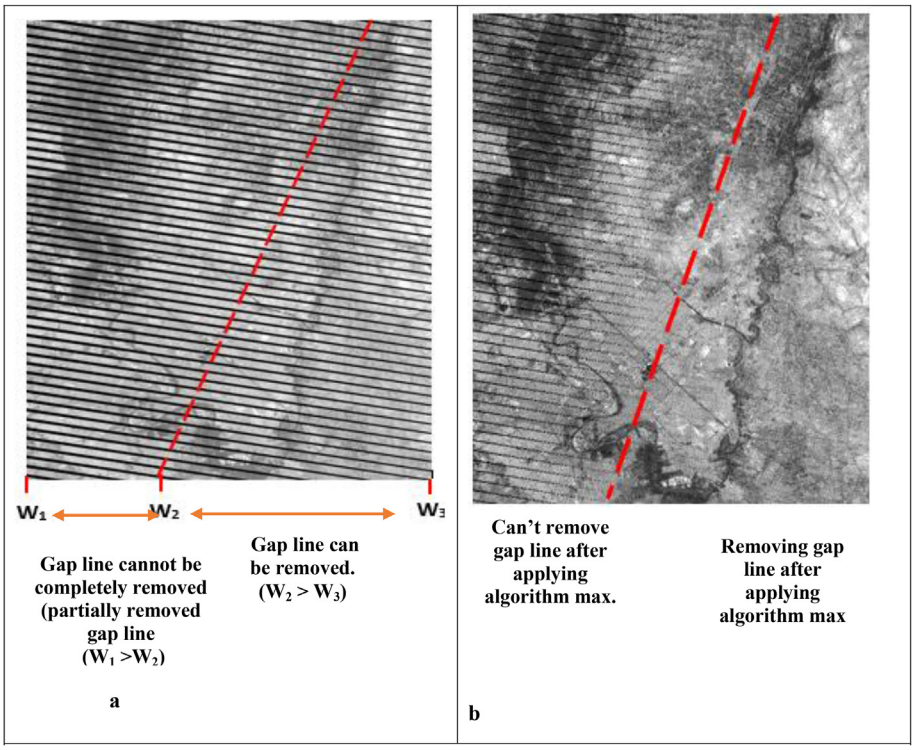

Fig. 3. a- The original image with the gaps, b-The result of the proposed algorithm for filling the gaps.

9. Enhance the output image using ETM+ (gap-free) [IN_{mean}, IN_{median}, and IN_{max}]

Suggested technology (mathematical model)

1 It is a continuation of the gap-filling process using (temporal filtering), this work is done after performing the temporal filtering technique, some of the resulting images will not be completely gap-free, leaving instead some narrow and unequal lines that are usually specific to the first third of the left side of the processed images, the maximum width of these lines can be up to 10 pixels.

2 The proposed technique is a continuation of the Temporal filtering process to obtain images free of gaps, where a linear filter will be applied in a perpendicular orientation to the images. The work steps are as follows:

a. Using B6 package or B6 for the purpose of locating the remaining gap lines.

b. Using a window in the form of a linear vector with a length of 11 pixels applied vertically in the region of the remaining gaps depending on the locations identified in point a where the non-zero points in this linear vector are located in the region of the remaining gaps, to get a new vector "v2" with a length Less than 11 pixels.

3 The window's center value (11) pixels is replaced by one of the following three values:

a. The mean for non-zero values (v2)

b. The median of non-zero values (v2)

c. The maximum window values (v2)

Thus, we get three filtered images for each case, as shown in the figure below. Using this technique, deals with the remaining gaps only, while the rest of the image points will not be affected.

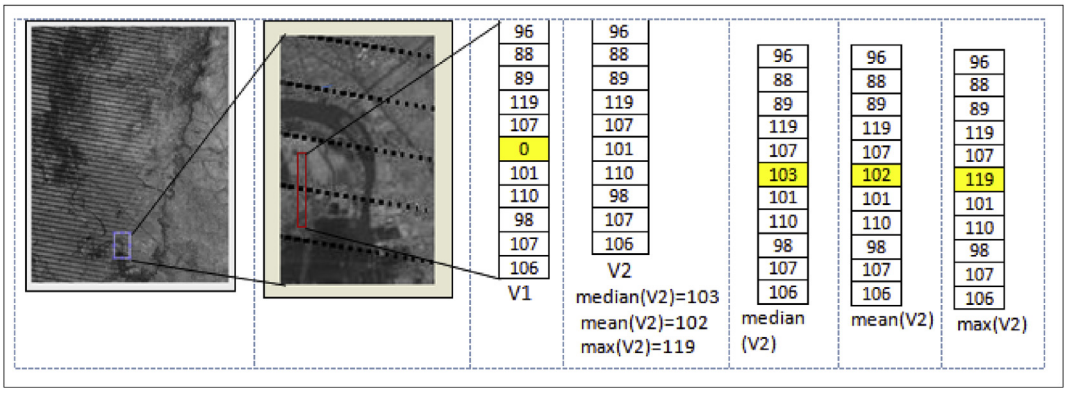

4. Results and discussion

This paper studies a gap-filling algorithm for the ETM+ imaging sensor based on the maximum value of the three-temporal satellite ETM imagery + taken over a period of 32-day. This technique succeeded in filling the gap where the line width is less than (upper and lower) pixels but failed when the line width was (W_1>W_2), therefore, in this study, another process was introduced to fill the ETM_+ - 2004 image gap by using

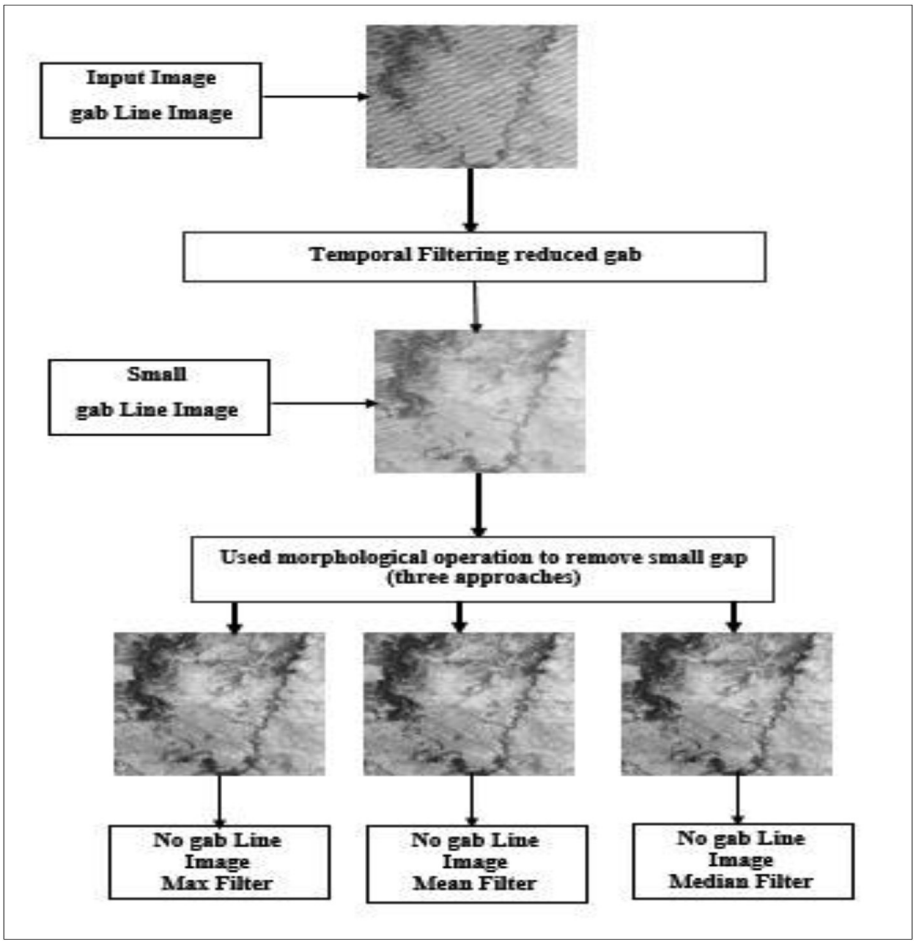

Fig. 4. Work plan.

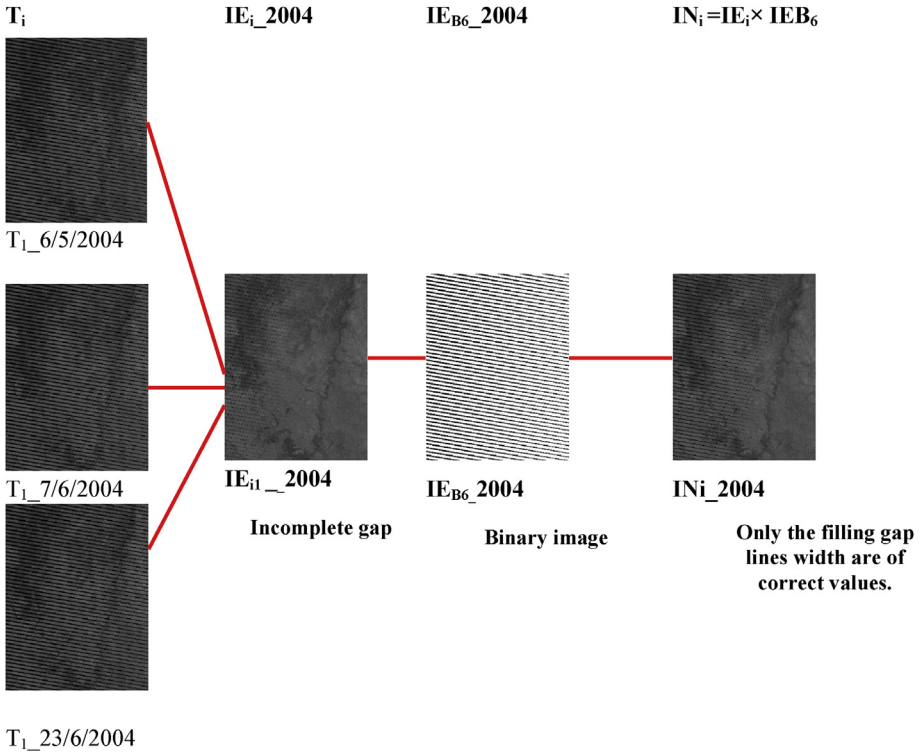

Fig. 5. The result of the extracted image containing only one gap line correctly.

linear and non-linear filters. Fig. (5) illustrated the extracted image containing only one gap line, and created a new image IN_i using:

$$IN_i = IE_{B6} \times IE_i$$

where i = 1, 2, 3,4,5,7.

The size of the image is the product of multiplying the number of rows and number of columns:

no. of rows x no. columns

i.e. 1263 x 1639.

The basic idea of this procedure is dealing with each image pixel in gap points as follows:

The pixel ($P_0 = 0$) in the image (IN_i) and the surrounding neighboring pixels (above and below P_0) are taken according to the vertical mask, then all the values are summed and divided by No. of elements (11 elements), which is the mean value. Finally, the old pixel is replaced with a new average value by filters and continues until the mean value replaces all pixels in the gap image. Fig. (6) shows the resulting image.

The **median filter** method is done by moving the pixel through the image pixels while replacing every value of the gap point ($P_0 = 0$ in image IN_i) by the median value of neighboring pixels (above and below P_0) according to the mask vertical. Fig. (6) shows the resulting image.

The **maximum filter** method is done by moving the pixel through the image pixel while replacing every value of the gap point ($P_0 = 0$ in image IN_i) with the maximum value of neighboring pixels (above and below P_0) according to the vertical mask. Fig. (6) shows the resultant image. ＼

the elapsed time is 8.965422 seconds (Max Filter)

the elapsed time is 9.692091 seconds (Mean Filter)

the elapsed time is 7.532509 seconds (Median Filter)

The results of similarity values using equation - 5- calculated as shown in Table (1):

To examine the quality of images resulting from the proposed algorithms, the NMSE Equation was modified as shown in Equation (6), applied to get normalized mean square error for the gap regions after applying the gap-filling algorithms.

$$NMSE_1 = \frac{1}{255^2}\sum_{i=1}^{N}\sum_{j=1}^{M}\left[\left(IN_{(i,j)} - IE_{(i,j)}\right)\right]^2 \quad (6)$$

where $NMSE_1$ represents a normalized mean square error, (N,M) row and column of image, IN=(INmean,

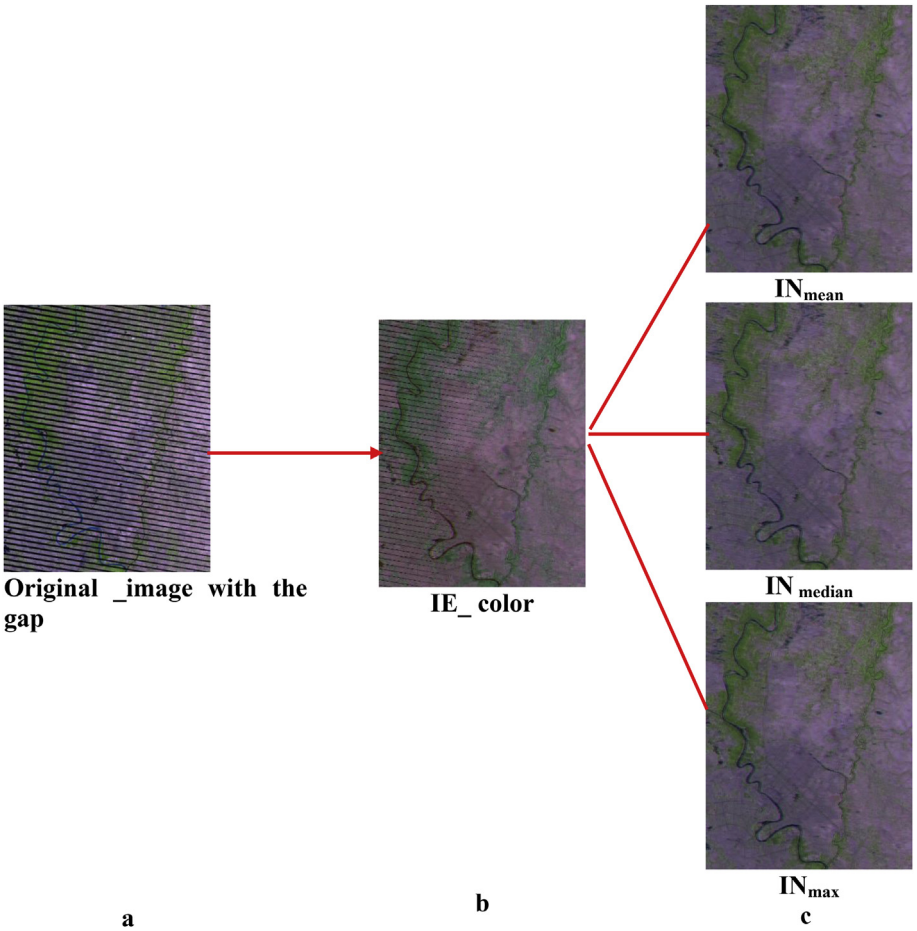

Fig. 6. a- Original image (1263 × 1639) pixel in size with gaps. b- Image enhancement ETM+ (gap reduction using three temporal images). c- Image enhancement ETM+ (gap free) using (maximum, mean and median) filters.

INmedian, and INmax) gap-free images, and IE is the gap line images, and the results are shown in Table (2).

The work in the proposed algorithms is done only in the gap regions, so that no error may occur in other regions of the image, and to demonstrate this, the normalized mean square error was calculated in non-gap regions (the regions of the image without gaps) before and after applying the gap-filling techniques, there were no noticeable changes in the normalized mean square error values.as shown in equation (7):

$$NMSE_2 = \frac{1}{255^2}\sum_{i=1}^{N}\sum_{j=1}^{N}\left[(IN \times IB_6)_{(i,j)} - (IE \times IB_6)_{i,j}\right]^2 \quad (7)$$

Table 1
The metric similarity value between the original band and image enhancement IE_i gap reduction and image enhancement (IN_{mean}, $IN_{median,}$ and IN_{max} gap-free) using (maximum, mean and median) filter (2004).

Bands	Jaccard original and IE_i	Jaccard IE_i and IN_{meani}	Jaccard IE_i and $IN_{i\ median}$	Jaccard IE_i and IN_{maxi}
B_1	0.6067	0.8434	0.8433	0.8118
B_2	0.6403	0.8470	0.8691	0.8427
B_3	0.6493	0.9007	0.9004	0.8820
B_4	0.7416	0.6274	0.6275	0.6026
B_5	0.6653	0.7685	0.7683	0.7439
B_7	0.7475	0.6568	0.6568	0.6246

Table 2
Shows the normalized mean square error between the input image IE and the resulting images from the gap-filling techniques IN.

(IN, IE)/(255^2)		
IN_{max}	IN_{mean}	IN_{median}
0.002872	0.0022026	0.00221007
0.003094	0.0022741	0.00228134
0.0051345	0.0036103	0.00363144
0.0045769	0.0034407	0.00346973
0.0061899	0.0044072	0.00444642
0.0185004	0.0155647	0.01556123
0.0309384	0.0271309	0.02726607
0.0309384	0.0271309	0.02726607

Table 3
Shows the normalized mean Square Error values for the non-gap-free areas before and after applying the gap-filling techniques.

($INXIB_6$, $IE \times IB_6$)/(255^2)		
$IN_{max}IB6$	$IN_{mean}IB_6$	$IN_{median}IB6$
1.87E-05	1.80E-05	1.80E-05
2.23E-05	2.05E-05	2.06E-05
3.32E-05	2.93E-05	2.97E-05
2.86E-05	2.62E-05	2.62E-05
3.93E-05	3.81E-05	3.84E-05
0.000658858	0.000549391	0.00055014
9.62E-05	9.70E-05	9.66E-05
9.62E-05	9.70E-05	9.66E-05

where $INxIB_6$ and $IExIB_6$ represent multiply the images IN=(INmean, INmedian, INmax) and IE by band 6 (only gap region), so the normalized mean square error calcolate only for non-gap regions, as shown in Table 3.

The (morphological) operations, which are (open - close, imdilate) are efficient in filling small gaps and the (temporal filtering) technique treated most of the areas and left only small gaps, these small gaps can be treated using (morphological) techniques as the (temporal filtering) technique but in some cases, they fail to leave small gaps, and the best way to fill these small gaps are the morphological techniques. After processing, these images can be analyzed and classified in new work projects.

5. Conclusions

In this study, three different ETM + time images with a 16-day interval between one image and the other were used to fill gap lines, complement the images, and minimize the effect of gaps. The used algorithm is based on using one of three filters (mean, median, and max.) to work on a vertical linear window (11px long vertically) whose center is on the points of the gap lines in the image. The gaps were completely removed, and the processing was done in the areas of the removed gaps only, which were very few, thus the processing was done without distorting any other part of the image. The mean square error criterion, as well as the Jaccard metric similarity index, were used to judge the significance of the method's results. In general, it is preferred to use the macroscopic tests done by experts and specialists in filling the gaps. From the results, the following points can be concluded:

1. The use of the temporal filtering method for ETM+ images to remove gap lines is not enough to completely remove gaps from Baghdad city images taken in 2004.
2. The results of applying spatial filtration to the images after using temporal filtration showed great effectiveness in removing gap lines from them. As the results of the three spatial filters (Median, Mode, and Maximum) indicated that they are effective for predicting unscanned pixels.
3. The results of the output images after removing the gap lines were good and the values of the Jaccard index were within the limits of (0–1). As the pictures preserved their actual values, and there were no changes in the gap-free areas. While the metric values for the gap line areas (0.6246–0.9007) were shown as information that was added to them as a result of the correction process using temporal and spatial filtering processes.
4. Visually, the best results were obtained from the (mean and median) filters, where the images maintained a high interconnection between the treated areas, the removed gaps, and their adjacent areas. The filter results also showed that the edges and changes in the image brightness were more connected. These results were followed by the (max.) filter.

This work is a continuation of a previous technique (temporal filtering) that was used to fill in the gaps as there were some defects in the previous temporal filtering technique for treating the gaps, so this technique was suggested to address these defects and fill the remaining gaps that the temporal filtering technique was unable to.

References

[1] Y. Gaohong, M. Gregoire, S. Ying, F. Matthew, A comparison of gap-filling approaches for Landsat-7 satellite data, Int. J. Rem. Sens. 23 (2017) 6653−6679.

[2] A. Ershadi, M.F. McCabe, J.P. Evans, J.P. Walker, Effects of spatial aggregation on the multi-scale estimation of evapotranspiration, Remote Sens. Environ. 131 (2013) 51−62.

[3] R. Houborg, M.F. McCabe, A. Cescatti, F. Gao, M. Schull, A. Gitelson, Joint leaf chlorophyll content and leaf area index retrieval from landsat data using a regularized model inversion system, Remote Sens. Environ. 159 (2015) 203−221.

[4] K. J Bormann, M.F. McCabe, J.P. Evans, Satellite based observations for seasonal snow cover detection and characterisation in Australia, Remote Sens. Environ. 123 (2012) 57−71.

[5] USGS, Phase 2 Gap-Fill Algorithm: SLC-Off Gap-Filled Products Gap-Fill Algorithm Methodology, 2011. Available online at: landsat. usgs. Gov/documents/L7S LC Gap Filled Method .2004 pdf 2.

[6] S.K. Maxwell, G.L. Schmidt, J.C. Storey, A multi- scale segmentation approach to filling gaps in Landsat ETM+SLC- off image, Int. J. Rem. Sens. 28 (2007) 5339−5356.

[7] M.J. Pringle, M. Schmidt, J.S. Muir, Geostatistical interpolation of SLC-off Landsat ETM+ images, ISPRS J. Photogrammetry Remote Sens. 64 (2009) 654−664.

[8] J. Chen, X. Zhu, J.E. Vogelmann, F. Gao, S. Jin, A Simple and effective method for filling gaps in landsat ETM+ SLC-off images, Remote Sens. Environ. 115 (2011) 1053−1064.

[9] C. Zeng, H. Shen, L. Zhang, Recovering missing pixels for Landsat ETM+ SLC-off imagery using multi-temporal regression analysis and a regularization method, Remote Sens. Environ. 131 (2013) 182−194.

[10] G. Mariethoz, P. Renard, Reconstruction of incomplete data sets or images using direct sampling, Math. Geosci. 42 (2010) 245−268.

[11] G. Yin, G. Mariethoz, M.F. McCabe, Gap-filling of landsat 7 imagery using the direct sampling method, Rem. Sens. 9 (2017).

[12] L. Malambo, C.D. Heatwole, A multitemporal profile-based interpolation method for gap filling nonstationary data, IEEE Trans. Geosci. Rem. Sens. 54 (2016) 252−261.

[13] P. Scaramuzza, E. Micijevic, G. Chander, SLC Gap-filled Products Phase One Methodology, 2018. Available online: https://doi.gov/2QEVyGy.

[14] S. Salema, H. Anwar, K.H. Heba, A. Al-Zuky Ali, Adaptive method for landsat ETM+ gap filling using successive temporal images, NeuroQuantology 18 (2020) 112−122.

[15] H. Akima, A method of bivariate interpolation and smooth surface fitting for irregularly distributed data points, ACM Trans. Math Software 2 (1978) 148−159.

[16] C. Zhang, W. Li, D. Travis, Gaps-fill of SLC-off Landsat ETM+ satellite image using a geostatistical approach, Int. J. Rem. Sens. 28 (2014) 5103−5122.

[17] R. Cooke, S. Mostaghimi, J.C. Parker, Estimating oil spill characteristics from oil heads in scattered monitoring wells, Environ. Monit. Assess. 28 (1993) 33−51.

[18] A. Nath, Image Denoising Algorithms: a comparative study of different filtration approaches used in image restoration, in: IEEE International Conference on Communication Systems and Network Technologies, 2013.

[19] S. Esakkirajan, T. Veerakumar, N. Adabala, C.H. PremChand, Removal of high-density salt and pepper noise through modified decision based unsymmetric trimmed median filter, IEEE Signal Process. Lett. 18 (2011) 287−290.

[20] Z. Tavor Baharav, M. Kamath Govinda, N. Tse David, Spectral Jaccard Similarity: A New Approach to Estimating Pairwise Sequence Alignments, Pattern cell press, 2020 open Access 11.